Soft Matter

PAPER

View Article Online
View Journal | View Issue

Cite this: *Soft Matter*, 2015, **11**, 1107

Cell membrane wrapping of a spherical thin elastic shell

Xin Yi and Huajian Gao*

Received 3rd November 2014
Accepted 9th December 2014

DOI: 10.1039/c4sm02427c

www.rsc.org/softmatter

Nanocapsules that can be tailored intelligently and specifically have drawn considerable attention in the fields of drug delivery and bioimaging. Here we conduct a theoretical study on cell uptake of a spherical nanocapsule which is modeled as a linear elastic solid thin shell in three dimensions. It is found that there exist five wrapping phases based on the stability of three wrapping states: no wrapping, partial wrapping and full wrapping. The wrapping phase diagrams are strongly dependent on the capsule size, adhesion energy, cell membrane tension, and bending rigidity ratio between the capsule and membrane. Discussion is made on similarities and differences between the cell uptake of solid nanocapsules and fluid vesicles. The reported results may have important implications for biomedical applications of nanotechnology.

1 Introduction

As a special class of nanoparticles with a solid shell and a hollow interior compartment, nanocapsules have found broad biomedical applications, especially as drug delivery vehicles with tunable geometrical, mechanical and physicochemical properties. These nanomaterials can be designed to release their encapsulated cargos in a controllable manner in response to external triggers such as temperature, pH, light, ionic strength, salt concentration and mechanical deformation.[1,2] Typical nanocapsules include polymeric capsules, polymeric micelles, colloidosomes[1,2] as well as viral capsids.[3,4] Although considerable effort has been dedicated to the mechanical stability of nanocapsules,[5,6] so far only a few theoretical[7] and experimental studies[8–10] have focused on their interactions with cells. It was found that cargos encapsulated in soft nanocapsules are released prematurely outside cells, while those in stiff capsules are fully delivered into cells,[9] and a two-dimensional theoretical study showed that full engulfment of soft nanocapsules requires stronger adhesion energy than that of stiff ones.[7] Besides these studies on cell uptake of nanocapsules, considerable interest has been paid to the elasticity effects in cell uptake of nanoparticles in general.[11–14] It was found that phagocytosis of soft microparticles is hindered by particle deformation.[11] Theoretical studies also indicated that stiff nanoparticles can be more easily engulfed than soft ones.[7,12] Molecular dynamics simulations demonstrated that nanoparticles grafted with stiffer ligands are more easily engulfed than those coated with softer ligands.[13]

So far, the existing theoretical studies on cell uptake of elastic nanoparticles have modeled the particles as fluid vesicles.[7,12] Due to the free lateral movement of lipid molecules and high resistance to lateral stretching, both vesicles and cell membrane can undergo substantial bending deformation in an Eulerian description. For cell uptake of a solid thin-shelled nanocapsule, the deformation of the cell membrane is described more easily in an Eulerian description but the deformation of the capsule prefers a Lagrangian description. A theoretical challenge thus exists in the coupling of Eulerian and Lagrangian descriptions. Here we perform the first theoretical study on cell uptake of a linear elastic thin-shelled nanocapsule. A numerical optimization approach is employed to tackle the Eulerian–Lagrangian coupling. It is investigated how the wrapping degree depends on the nanoparticle size, adhesion energy, membrane tension, and bending rigidity ratio between the capsule and membrane. A wrapping phase diagram of cell-nanocapsule interaction is established to probe the transitions between no wrapping, partial wrapping, and full wrapping states. Moreover, discussion is made on similarities and differences between the cell uptake of the solid thin-shelled nanocapsule and fluid vesicle. Possible implications of our results for therapeutic drug delivery are also discussed.

2 Model and methods

The elastic nanoparticles in the existing theoretical studies on cell uptake have been modeled as elastic lipid vesicles deforming *via* lateral lipid movement under the energetic cost of bending and constraint of surface area conservation.[7,12] In two dimensions (2D), a cylindrical capsule with an inextensible elastic thin shell undergoes a pure bending deformation. Therefore, the wrapping of a 2D inextensible elastic thin shell

School of Engineering, Brown University, Providence, Rhode Island 02912, USA. E-mail: huajian_gao@brown.edu

capsule by a lipid membrane is mathematically equivalent to that of a 2D elastic cylindrical vesicle with a given cross-sectional circumference.[7] In three dimensions (3D), there is no longer such equivalence between vesicles and solid capsules, since the deformation of a solid thin-shelled capsule requires not only bending but also in-plane stretching of the shell. For capsules made of linear elastic materials, the cost of stretching is significant. The high energetic cost of stretching prevents the formation of cylindrical tether structures commonly observed in lipid bilayer membranes subject to a point force.[15]

We consider the adhesive wrapping of a spherical thin-shelled capsule undergoing an axisymmetric deformation by a lipid membrane in the adopted cylindrical coordinate (r, ϕ, z) (Fig. 1). Since the axisymmetric deformation of the capsule and membrane is independent of the circumferential coordinate ϕ and there is no in-plane shear deformation, we restrict our attention to a certain vertical cross-section of the configuration (*e.g.*, $\phi = 0$). Before it contacts the membrane, the capsule in the stress-free state is assumed to take a spherical shape of radius a as its reference configuration (Fig. 1b). A material point at $(r = r_0, z = z_0)$ in the undeformed reference configuration can be generally parameterized by the curvilinear coordinates $s_0 \in [0, L_0]$ and $\psi_0 \in [0, \pi]$ with geometrical relationships

$$\mathrm{d}r_0/\mathrm{d}s_0 = \cos\psi_0 \quad \text{and} \quad \mathrm{d}z_0/\mathrm{d}s_0 = \sin\psi_0,$$

where s_0 is the arc length measured along the meridian from the bottom pole in the reference configuration, L_0 denotes the half

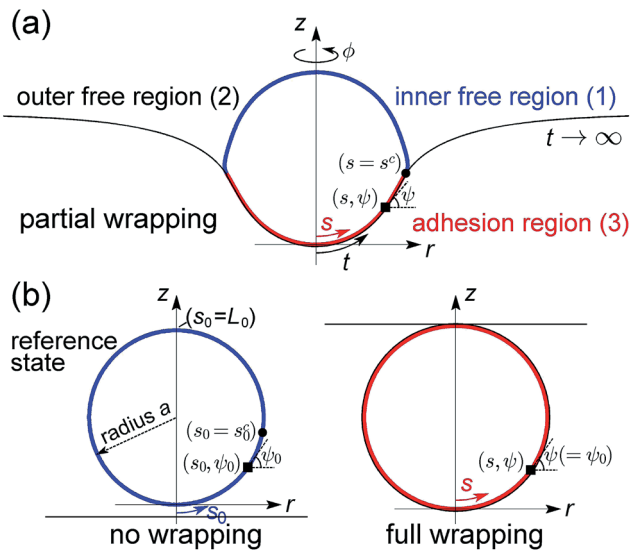

Fig. 1 Schematic of an elastic thin-shelled spherical capsule (thick line) of initial radius a wrapped by an initially flat cell membrane (thin black line) in the adopted cylindrical coordinate (r, ϕ, z). (a) The geometry of the system with tangent angle ψ. Arc lengths s and t are defined along the capsule and membrane, respectively, measured from the bottom pole ($s = t = 0$). (b) Schematic for the states of no wrapping (stress-free reference state) with zero contact region and full wrapping in which the capsule is fully wrapped by the membrane. Partial wrapping corresponds to an intermediate scenario with incomplete wrapping as shown in (a).

of the circumference of the cross-section, and ψ_0 is the tangent angles. The surface area is $A_0 = 2\pi \int_0^{L_0} r_0 \mathrm{d}s_0$. The principal curvatures at point (s_0, ψ_0) in the meridional (longitudinal) and circumferential (latitudinal) directions are

$$c_{s_0} = \mathrm{d}\psi_0/\mathrm{d}s_0 \quad \text{and} \quad c_{\phi_0} = \sin\psi_0/r_0.$$

For the spherical capsule under consideration, we have $L_0 = \pi a$, $\psi_0 = s_0/a$, $r_0 = a \sin\psi_0$, $z_0 = a(1 - \cos\psi_0)$, and $c_{s_0} = c_{\phi_0} = 1/a$. Hereinafter a subscript 0 without specific notifications is used to identify a quantity associated with the reference state.

As the membrane wraps around the capsule, the wrapping state evolves from the state of no wrapping (defined as the reference state in Fig. 1b) to partial wrapping (Fig. 1a). In the state of partial wrapping, the material point (s_0, ψ_0) located at (r_0, z_0) is displaced by the membrane to (r, z) with curvilinear coordinates (s, ψ) in the deformed configuration where the deformation field can be characterized by longitudinal stretch λ_s and latitudinal stretch λ_ϕ in the meridional and circumferential directions, respectively, as

$$\lambda_s = \mathrm{d}s/\mathrm{d}s_0 \quad \text{and} \quad \lambda_\phi = r/r_0.$$

Without loss of generality, we consider a capsule made of a linearly elastic isotropic thin shell of thickness h. Its strain energy density W_s is[5,6,16]

$$W_s = \frac{Eh}{2(1-\nu^2)}\left(e_s^2 + 2\nu e_s e_\phi + e_\phi^2\right) + \frac{D}{2}\left(C_s^2 + 2\nu C_s C_\phi + C_\phi^2\right), \tag{1}$$

where E is Young's modulus, $\nu \in [-1, 1]$ is the Poisson ratio of the shell, and

$$e_s = \lambda_s - 1 \quad \text{and} \quad e_\phi = \lambda_\phi - 1$$

are the meridional and circumferential strains, respectively; $D = Eh^3/[12(1-\nu^2)]$ is the bending rigidity of the thin shell, and C_s and C_ϕ are the meridional and circumferential bending strains, respectively,

$$C_s = \lambda_s c_s - c_{s_0} \quad \text{and} \quad C_\phi = \lambda_\phi c_\phi - c_{\phi_0},$$

with the meridional curvature $c_s = \mathrm{d}\psi/\mathrm{d}s$ and circumferential curvature $c_\phi = \sin\psi/r$.

The elastic energy density of the deformed cell membrane is[12,17,18]

$$W_\mathrm{m} = \frac{\kappa_\mathrm{m}}{2}\left(c_s^{(\mathrm{m})} + c_\phi^{(\mathrm{m})}\right)^2 + \sigma(1 - \cos\psi_\mathrm{m}), \tag{2}$$

where κ_m, $c_s^{(\mathrm{m})} = \mathrm{d}\psi_\mathrm{m}/\mathrm{d}t$, $c_\phi^{(\mathrm{m})} = \sin\psi_\mathrm{m}/r$, ψ_m, and t are the bending stiffness, meridional curvature, circumferential curvature, tangent angle, and arc length of the cell membrane, respectively. With eqn (1) and (2) the total energy of the system is

$$E_\mathrm{tot} = \int_0^{L_0} 2\pi r_0 W_s \mathrm{d}s_0 + \int_0^{\infty} 2\pi r W_\mathrm{m} \mathrm{d}t - \gamma A_3,$$

where γ is the adhesion energy representing the specific adhesive interaction between the nanocapsule and cell membrane, and $A_3 = \int_0^{s^c} 2\pi r ds$ is the contact area with $s = s^c$ as the arc length at the contact edge. The contact edge corresponds to arc length position $s_0 = s_0^c$ in the reference configuration. The wrapping degree f for a certain wrapping state is defined as

$$f = \int_0^{s_0^c} 2\pi r_0 \mathrm{d}s_0 / A_0,$$

i.e. the corresponding area of the contact region in the reference configuration divided by the total surface area A_0 of the undeformed capsule.

Here we employ a numerical optimization technique to determine the minimum energy state at each given wrapping degree f. With geometric relations $\mathrm{d}r/\mathrm{d}s = \cos\psi$ and $\mathrm{d}z/\mathrm{d}s = \sin\psi$, the deformation of the capsule as well as the membrane attaching on it is determined by the tangent angle ψ and the longitudinal stretch $\lambda_s = \mathrm{d}s/\mathrm{d}s_0$, while the shape of the outer free membrane is determined by the tangent angle ψ. The tangent angle ψ and longitudinal stretch λ_s in the inner free region are approximated by cubic B-spline functions as[7,19]

$$\psi(a^{(1)}, s_0) = \sum_{i=0}^{n} a_i^{(1)} N_i(s_0) \quad \text{and} \quad \lambda_s(b^{(1)}, s_0) = \sum_{i=0}^{n} b_i^{(1)} N_i(s_0).$$

Similar forms based on cubic B-spline are employed for $\psi_m(a^{(2)}, t)$ in the outer free region and $\psi(a^{(3)}, s_0)$ and $\lambda_s(b^{(3)}, s_0)$ in the adhesion region. Here superscripts (1), (2) and (3) identify quantities associated with the inner free, outer free, and wrapped regions, respectively (Fig. 1). Control points a_i and b_i are coefficients of the cubic basis functions N_i with integer indices $0 \le i \le n$. The basis functions $N_i(s_0)$ and $N_i(t)$ can be determined explicitly by specifying knot vectors of the variable parameters s_0 and t, respectively. A typical choice of the knot vector for a parameter $\xi \in [p, q]$ is taken as $\{\xi_0, \ldots, \xi_{n+4}\}$ with $\xi_i = p$ $(i = 0, \ldots, 3)$ and $\xi_i = q$ $(i = n+1, \ldots, n+4)$. Here n is chosen as $n = 68$.

The boundary and constraint conditions provide either input parameters or equality constraints during energy minimization. As $t \to \infty$, the outer free membrane becomes asymptotically flat which requires $\psi_m|_{t\to\infty} = 0$ or $a_n^{(2)} = 0$. Similarly, $\psi|_{s_0=L_0} = \pi$ and $\psi|_{s_0=0} = 0$ require $a_n^{(1)} = \pi$ and $a_0^{(3)} = 0$, respectively. At the contact edge $s = s^c$ (or $s_0 = s_0^c$), the continuity of the tangent angle requires $a_0^{(1)} = a_n^{(3)} = a_0^{(2)}$. The continuity of the coordinate (r, z) at the contact edge is enforced as equality constraints. The total energy E_{tot} as a function of $\psi(s_0)$, $\lambda_s(s_0)$ and $\psi_m(t)$ under these constraints at a given f and adhesion energy γ is minimized with respect to the control points a_i and b_i using the interior point method.[20] Once the tangent angles ψ and ψ_m and the longitudinal stretch λ_s are known, the total energy and corresponding shapes of the capsule and membrane can be determined.

At the full wrapping state ($f = 1$), the spherical capsule with initial radius a deforms into a sphere of radius ρ. In that state, $\lambda \equiv \lambda_s = \lambda_\phi = \rho/a$, $e_s = e_\phi = \lambda - 1$, and $C_s = C_\phi = 0$, and $W_s = Eh(\lambda - 1)^2/(1 - \nu)$. Since the membrane elastic energy of the outer free region at full wrapping is negligible compared to the elastic energy of membrane adhering on the capsule,[12,18] the total energy of the system at full wrapping can be approximated as the sum of the adhesion energy and the elastic energy of the capsule and adhering membrane, *i.e.*

$$E_{tot} \approx 4\pi a^2 \frac{Eh}{(1-\nu)}(\lambda - 1)^2 + 2\pi\lambda^2\kappa_m(\bar{\sigma} - \bar{\gamma}) + 8\pi\kappa_m,$$

where $\bar{\sigma} \equiv 2\sigma a^2/\kappa_m$ is the normalized membrane tension and $\bar{\gamma} \equiv 2\gamma a^2/\kappa_m$ the normalized adhesion energy. Letting $\mathrm{d}E_{tot}/\mathrm{d}\lambda = 0$ gives

$$\lambda = \frac{2Ea^2h}{2Ea^2h + \kappa_m(\bar{\sigma} - \bar{\gamma})(1-\nu)}.$$

The necessary condition for a stable state of full wrapping is $E_{tot} < 0$ (or $\bar{\gamma} > \bar{\sigma}$), which means that $\lambda > 1$ or the spherical capsule is enlarged through interactions with the membrane.

3 Results

To investigate the effects of capsule elasticity on cell uptake, we consider elastic capsules with various bending rigidity $D = Eh^3/[12(1 - \nu^2)]$. Hereinafter we take $\nu = 0.4$ and $h = 0.05a$, where a is the radius of the spherical capsule in the reference configuration. Fig. 2a shows the elastic energy change $\Delta E_{el} = E_{el} - E_{el}^0$ as a function of the wrapping degree f for different D/κ_m at $\bar{\sigma} = 2$ and $\bar{\gamma} = 0$, where $E_{el} \equiv E_{tot} + \gamma A_3$ is the

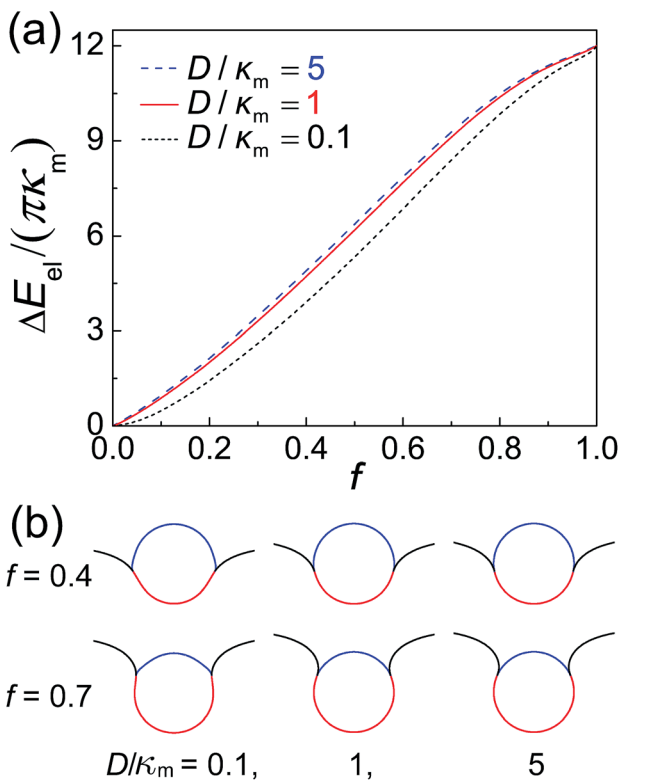

Fig. 2 (a) Elastic energy ΔE_{el} as a membrane wraps around an elastic thin-shelled capsule with wrapping degree f for different D/κ_m at $\bar{\sigma} = 2$ and $\bar{\gamma} = 0$. (b) Selected wrapping configurations at $\bar{\sigma} = 2$ and $\bar{\gamma} = 9$ for different stiffness ratios D/κ_m.

elastic energy of the system and E_{el}^0 is the reference energy before the capsule contacts the membrane. Here $E_{el}^0 = 0$ since the reference state in the current study is stress-free. For capsules with a pre-stress or eigenstrain field, E_{el}^0 could have a non-zero value depending on the definition of the reference state. As the stiffness ratio D/κ_m decreases, the slope $d(\Delta E_{el})/df$ decreases in the early stage of wrapping and increases in the late stage, indicating that the wrapping around softer capsules requires smaller adhesion energy in the early wrapping stage but larger adhesion energy in the late stage. Wrapping around a stiff capsule involves a gentle rise in the elastic energy as the cell membrane deforms gradually around the capsule. For a soft particle, the elastic deformation energy is partitioned between the capsule and the membrane as illustrated in Fig. 2b. A very soft capsule would initially spread along the membrane without inducing significant membrane deformation. Only at a later stage will the membrane be forced to bend around the capsule and catch up to almost the same configuration at full wrapping as in the case of a stiff capsule. This means a more abrupt rise in elastic energy at the later stage of wrapping for soft capsules. A similar phenomenon has been observed in the membrane wrapping of elastic vesicular particles.[12] Here only the energy profiles at $\bar{\gamma} = 0$ are provided. Further numerical results indicate that $\bar{\gamma}$ of practical interest has negligible influence on the elastic energy profiles due to the slight area dilatation in the contact region which is attributed to the high cost of stretching a solid thin shell. For thin shells made of hyperelastic materials with low cost of stretching, $\bar{\gamma}$ would play a more important role in the evolution of elastic energy. Fig. 2b shows sequences of wrapping configurations at $\bar{\sigma} = 2$ and $\bar{\gamma} = 9$ for different stiffness ratios D/κ_m. The softer the capsule is, the larger the capsule deformation is induced by the wrapping membrane.

The total energy difference $\Delta E = E_{tot} - E_{el}^0$ corresponds to the sum of the elastic energy difference ΔE_{el} and adhesion energy $-\gamma A_3$. Fig. 3 shows ΔE as a function of the wrapping degree f for different $\bar{\gamma}$ and D/κ_m at $\bar{\sigma} = 2$. The behavior of ΔE indicates that there exist five possible phases. We focus on relatively stiff capsules (*e.g.*, $D/\kappa_m = 5$) first. For small adhesion energy $\bar{\gamma}$, ΔE increases monotonically with f and no wrapping (phase I) prevails. As $\bar{\gamma}$ increases, phase II comes into existence in which a stable state of no wrapping and a metastable state of partial wrapping coexist. Further increase in $\bar{\gamma}$ results in a global minimum at a state of partial wrapping and an energy barrier to reach the (metastable) state of full wrapping (phase III). Next we encounter phase IV in which the stable state of partial wrapping becomes metastable while the full wrapping state becomes stable. Eventually, if $\bar{\gamma}$ is large enough, phase V arises where the energy barrier to full wrapping vanishes and the latter becomes the only stable state. For each phase, there is a stable state of a global energy minimum and possibly a metastable state of a local energy minimum. For relatively soft capsules (*e.g.*, $D/\kappa_m = 1$ and 0.1), the adhesion energy can compensate for the bending energy at initial wrapping, and phase II is replaced by II′. Depending on the values of $\bar{\sigma}$ and $\bar{\gamma}$, the energy profile ΔE of phase II′ could exhibit either one or two local energy minima. Similar behaviors shown in Fig. 3 have been observed in the membrane wrapping of vesicles.[12]

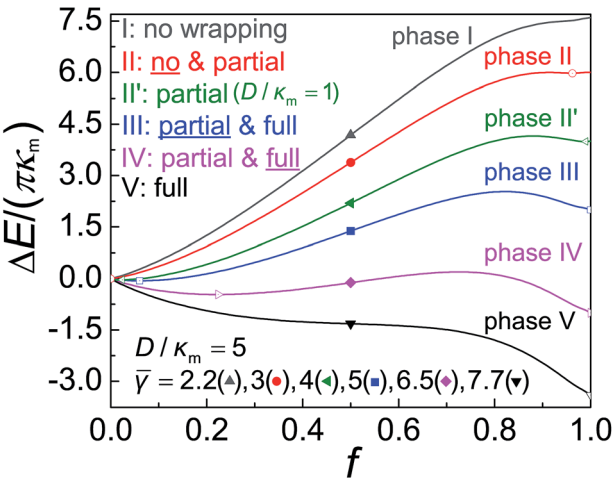

Fig. 3 Total energy change ΔE as a function of the wrapping degree f for different $\bar{\gamma}$ and D/κ_m at $\bar{\sigma} = 2$. The open symbols correspond to the local energy minima. Based on the stability of no wrapping, partial wrapping and full wrapping states, there exist five possible wrapping phases, two stable (I and V) and three metastable phases (II or II′ (depending on the value of D/κ_m) to IV). The underlined wrapping states in these metastable phases are the ones with lower energy. Phase I, a stable no wrapping state with a single energy minimum at $f = 0$; phase II, coexistence of a stable no wrapping state and a metastable partial wrapping state; phase III, coexistence of partial (stable) and full (metastable) wrapping states; phase IV, coexistence of metastable partial and stable full wrapping states; phase V, a stable full wrapping state with a single energy minimum at $f = 1$; phase II′, a stable partial wrapping state.

With the knowledge of energy profiles at different D/κ_m, $\bar{\sigma}$, and $\bar{\gamma}$, the phase diagrams of wrapping are determined and shown in Fig. 4. The full wrapping condition is taken as $f = 1$. For rigid capsules, the minimum adhesion energy necessary for partial wrapping is $\bar{\gamma}_{min} = 4$.[12,18] As D/κ_m decreases, $\bar{\gamma}_{min}$ decreases because softer capsules can be easily flattened in adhesion with the membrane; however, $\bar{\gamma}$ needs to rise sharply in the late stage to attain full wrapping. This conclusion can also be reached by comparing slopes of the elastic energy profiles in Fig. 2a where the energy curve for softer capsules (*i.e.* smaller D/κ_m) exhibits a smaller slope around $f = 0$ and a larger slope around $f = 1$ compared to that of stiffer ones. The phase diagrams shown in Fig. 4 indicate that stiffer capsules can attain full wrapping more easily than softer ones. This generic conclusion is also valid for vesicular nanoparticles.[12]

The elastic effects on the capsule deformation can be characterized by the longitudinal stretch λ_s and latitudinal stretch λ_ϕ. Fig. 5 shows λ_s and λ_ϕ of elastic capsules as a function of the normalized reference arc length $s_0/(\pi a)$ at $\bar{\sigma} = 2$ and $\bar{\gamma} = 6$. It is seen that the thin shell structure near the contact edge is under longitudinal compression and latitudinal stretching. The latitudinal stretching results from the flattening of the curved shell, which in turn leads to longitudinal compression to reduce the area dilatation and hence save stretching energy. As the capsule becomes soft and easily deformed, the region under longitudinal compression and latitudinal stretching enlarges with increasing extent of deformation. In Fig. 5, the results are

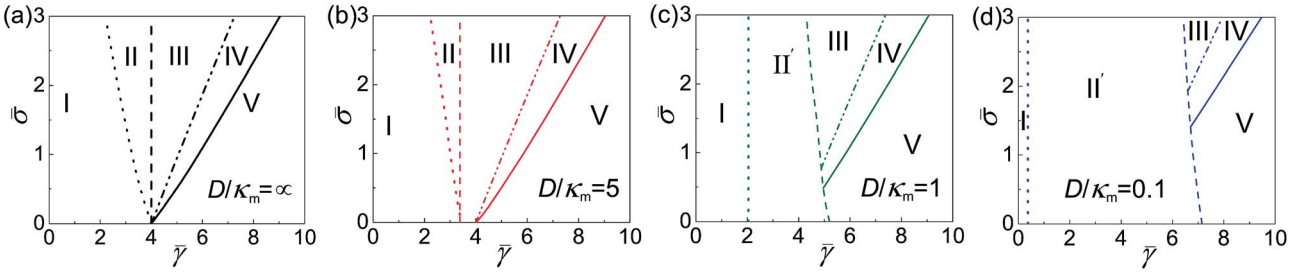

Fig. 4 Wrapping phase diagrams with respect to normalized adhesion energy $\bar{\gamma}$ and surface tension $\bar{\sigma}$ for $D/\kappa_m = \infty$, 5, 1 and 0.1. Dotted lines indicate boundaries between phases I and II (II′); dashed lines represent boundaries between phases II or II′ and III (as well as IV and V for $D/\kappa_m = 1$ and 0.1); dash-dotted lines are boundaries between phases III and IV; solid lines serve as boundaries between phases IV and V. The definition of phases I to V is referred to as in Fig. 3.

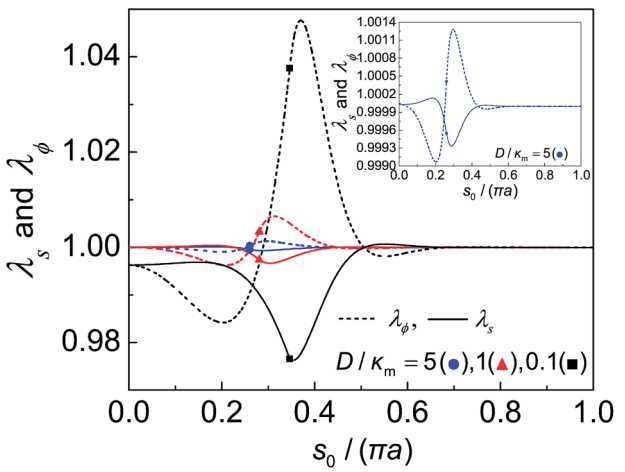

Fig. 5 The longitudinal stretch λ_s and latitudinal stretch λ_ϕ for elastic capsules with $D/\kappa_m = 5$, 1 and 0.1 at $\bar{\sigma} = 2$ and $\bar{\gamma} = 6$. The solid symbols indicate contact edge positions of the corresponding state of minimum energy in the reference configuration. Inset, zoom-in plot of λ_s and λ_ϕ for the case of $D/\kappa_m = 5$.

shown only for $s_0^c/(\pi a) < 0.5$ but a similar phenomenon exists for $s_0^c/(\pi a) > 0.5$.

Previous theoretical studies on the adhesion of a spherical thin elastic shell on a flat rigid substrate indicate that strong long-range adhesive interactions can induce a stable buckled state in which the central part of the adhesion region of the shell buckles away from the substrate, the so-called curvature-inversion buckling;[21,22] while this phenomenon is not observed in the case of short-range[21] or weak long-range adhesive interactions.[22] In our model, the specific adhesive interaction between the nanocapsule and membrane is characterized by a contact potential with vanishing interaction range, a limiting case of short-range adhesive interactions. Therefore, the curvature-inversion buckled state cannot be appropriately addressed by the current model. Besides the possible curvature-inversion buckling, the adhesive interaction might also induce wrinkling in the shell near the contact edge, as observed in the capillary wrinkling of thin films.[23,24] It will be interesting to conduct a thorough theoretical analysis of these issues in the future.

In addition to nanocapsules, vesicular nanoparticles such as liposomes serving as another important type of soft particles have also attracted much attention in the fields of drug delivery and diagnostics.[25] It may be interesting to compare the membrane wrapping of spherical vesicles investigated in our previous study[12] with that of a linear elastic solid thin-shelled capsules in the present study. The elastic energy density of axisymmetric vesicles with a given surface area but no constraints on volume or osmotic pressure is given as

$$W_v = \frac{\kappa_v}{2}\left(c_s^{(v)} + c_\phi^{(v)} - c_0^{(v)}\right)^2, \quad (3)$$

where κ_v, $c_s^{(v)}$, $c_\phi^{(v)}$, and $c_0^{(v)}$ are the bending stiffness, meridional curvature, circumferential curvature, and spontaneous curvature of the vesicle, respectively. In eqn (3) we have omitted the energy contribution from the Gaussian curvature of the vesicle since it does not affect the vesicle shape according to the Gauss–Bonnet theorem.[26] Thus, the total energy is

$$E_{tot} = \int 2\pi r(W_v + \Sigma_v)ds_v + \int_0^\infty 2\pi r W_m dt - \gamma A_3, \quad (4)$$

where Σ_v is a Lagrange multiplier to enforce the conserved total surface area of the vesicle, and s_v is the arc length measured along the meridian from the bottom pole of the vesicle. The governing equations of the system energy in eqn (4) can be determined by using variational methods, which together with boundary conditions are then solved *via* shooting methods.[12]

Here we consider vesicles with two illustrative spontaneous curvatures: zero spontaneous ($c_0^{(v)} = 0$) and $c_0^{(v)} = 2/a$, with a being the initial radius of the vesicle. In the first case, the vesicle before contact has a ground energy of $8\pi\kappa_v$; while in the latter case, the ground energy is zero, the same as the solid capsule considered here. Fig. 6 plots the elastic energy change $\Delta E_{el} = E_{el}^{(v,m)} - E_{el}^0$ as a function of the wrapping degree f for different κ_v/κ_m at $\bar{\sigma} = 2$, where $E_{el}^{(v,m)}$ is the elastic energy of the deformed vesicle and wrapping membrane and E_{el}^0 is the ground energy before the vesicle comes in contact with the membrane. The normalized membrane tension here is still defined as $\bar{\sigma} \equiv 2\sigma a^2/\kappa_m$. In contrast to solid capsules, ΔE_{el} values of vesicles are independent of γ due to the constraint of a constant area. For vesicles with $c_0^{(v)} = 0$, ΔE_{el} is slightly higher than those with $c_0^{(v)} = 2/a$. As κ_v/κ_m decreases, the slope of the

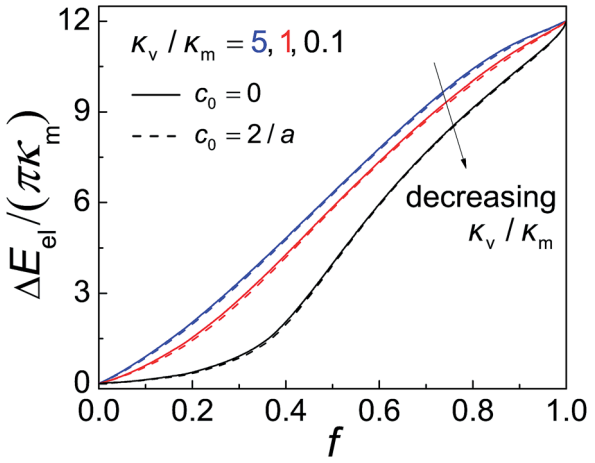

Fig. 6 Elastic energy change ΔE_{el} as a membrane wraps around a vesicular particle ($c_0^{(v)} = 0$ or $2/a$) with wrapping degree f for different κ_v/κ_m at $\bar{\sigma} = 2$ and $\bar{\gamma} = 0$.

energy profiles around $f = 0$ decreases and that around $f = 1$ increases. This means that softer vesicle particles require less $\bar{\gamma}_{min}$ to achieve partial wrapping but need higher $\bar{\gamma}$ to attain full wrapping. This is qualitatively similar to the case of solid capsules (see Fig. 2a).

For an isolated vesicle, the bending stiffness κ_v serves as the single material property governing its elastic deformation; while for an isolated solid capsule made of an isotropic linear elastic shell, its deformation depends on two independent material properties: the Poisson ratio ν and bending rigidity D. Although the energy dependence on the bending rigidity D for solid capsules and that on the bending stiffness κ_v in eqn (3) for vesicles have different forms, D does represent the ability to resist bending deformation and can be used to measure the softness of an elastic capsule as κ_v does for a vesicle, especially recalling that isotropic linear elastic thin shells typically exhibit a low degree of stretching. Since solid capsules considered here have zero elastic energy before contact, we compare vesicles with $c_0^{(v)} = 2/a$ with solid capsules at $\bar{\sigma} = 2$ in Fig. 7a–c. At $\kappa_v = D$, the energy profiles of the vesicle are lower than those of the solid capsule. Note that the wrapping degree f of a vesicle is defined as the area ratio between the contact region and the whole vesicle in the deformed state.[12] As particles become softer, the difference in ΔE_{el} between capsules and vesicles becomes larger. Compared to soft capsules with $D/\kappa_m = 0.1$, vesicles with $\kappa_v/\kappa_m = 0.1$ exhibit a larger region with a gentle slope in the early wrapping stage, which results from spreading of the vesicle along the membrane. This indicates that soft vesicles require a lower $\bar{\gamma}_{min}$ to attain partial wrapping than soft capsules of comparable bending stiffness. Since the vesicles exhibit similar trends of ΔE_{el} to solid capsules, it is not surprising that the wrapping phase diagrams of vesicular particles (see Fig. 3b–e in ref. 12) show similar structures to those of thin-shelled solid capsules (Fig. 4a–d). However, the lower energy profiles of vesicles compared to those of solid capsules indicate that under comparable bending rigidity, fluid vesicles would behave as softer capsules in their interactions with cells.

4 Discussion

The capsids of spherical viruses with icosahedral symmetry[3,4] and synthetic colloidosomes and polymeric capsules with spherical geometry[1,2] can be considered as typical nanocapsules. Their bending rigidity D and size can vary considerably. Here we give a few examples of viral capsids whose geometry and mechanical properties have been quantitatively characterized experimentally and theoretically, and then compare their bending rigidity D with that of the cell membrane, κ_m, which falls in a wide range from 20 k_BT (1 $k_BT = 4.11 \times 10^{-21}$ J) to 150 k_BT depending on the membrane composition.[27] For example, $\kappa_m = 20\ k_BT$ for the egg yolk phosphatidylcholine, $\kappa_m = 30\ k_BT$ for pure dimyristoyl phosphatidylcholine (DMPC) lipid bilayers, and κ_m of the DMPC membrane containing 50 mol% cholesterol is as high as $150\ k_BT$ at 30 °C.[27] For representative spherical viruses, the capsid radius a varies from 10 nm to 75 nm,[3] the Young's modulus E falls in the range of 100 MPa to a few (2 to 4) GPa, the average or effective thickness h of the capsids is about 1.6 nm to 5 nm, and the Poisson ratio ν is suggested to be 0.4.[4] Representative viruses with capsids of bending stiffness D comparable to κ_m include the hepatitis B virus (HBV), cowpea chlorotic mottle

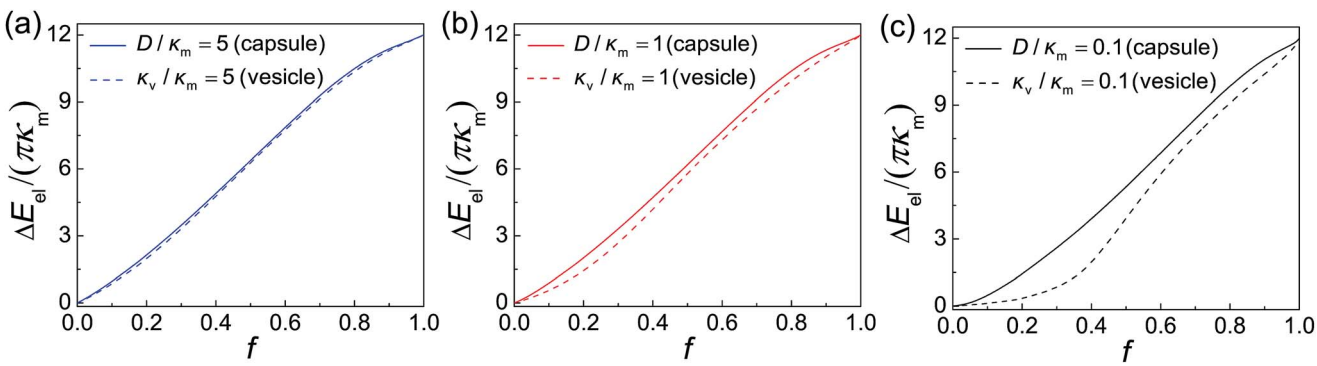

Fig. 7 Comparison of ΔE_{el} at $\bar{\sigma} = 2$ between the membrane wrapping of a capsule at $\bar{\gamma} = 0$ and a vesicle with $c_0^{(v)} = 2/a$ at different stiffness ratios D/κ_m (or κ_v/κ_m) as (a) 5, (b) 1, and (c) 0.1.

virus (CCMV), and bacteriophage λ (see Table 1).[4] It has also been reported that influenza virions exhibit a higher but comparable stiffness with respect to egg phosphatidylcholine liposomes.[28] For these nanocapsules, elasticity might play an important role in cell membrane wrapping. Representative viruses whose capsids are much stiffer than the cell membrane include the minute virus of mice (MVM),[4] mature human immunodeficiency virus (HIV),[29] herpes simplex virus type 1 (HSV1)[4] and mature murine leukemia virus (MLV)[30] (see Table 1). These viruses can be considered as rigid particles compared to the cell membrane. In addition to biological nanocapsules, it might be feasible to produce engineered nanocapsules as soft as cell membranes through, *e.g.*, synthesis of polymeric nanocapsules fabricated with ultra-soft materials such as polydimethylsiloxane (PDMS) whose Young's modulus E is in the range of 0.57 MPa to 3.7 MPa.[31] It has been reported that polymeric nanocapsules and lipid-core nanocapsules prepared with a mixture of organic compounds exhibit a low Young's modulus E on the order of 0.1 MPa.[32] Other soft engineered nanocapsules may include spherical nanostructures made of single-layered graphene ($D = 56.2\ k_BT$)[33] or hexagonal boron-nitride ($D = 37\ k_BT$).[34]

To reduce membrane bending and tension energies in cell interactions with a soft nanoparticle, the particle usually flattens and spreads along the wrapping membrane. In the case of thin-shelled solid capsules, the flattening and spreading of the adhesion region are mainly associated with stretching and bending of the shell. For a linear elastic thin shell of thickness h, the stretching energy scales as $\sim h$ and the bending energy as $\sim h^3$. Therefore, the thin-shelled capsule displays substantial bending deformation with slight expansion, as indicated in Fig. 2b and 5. Further bending deformation would cause considerable latitudinal stretching and longitudinal compression, which in turn results in significant stretching energy as analyzed in Fig. 5. In the case of a vesicular particle whose stretching modulus is much larger than its bending modulus, the total surface area of the vesicle is approximately conserved and the stretching energy is negligible. In addition, lipid molecules are free to move laterally in the bilayer. Thus, even with significant spreading of the vesicle along the membrane, no stretching energy arises and only bending energy results from the flattening of the adhered vesicle. Due to the fluidity of lipid membranes and consequent zero stretching energy, vesicles under membrane wrapping can achieve substantially higher bending deformation compared to solid capsules at comparable bending rigidities.

Table 1 Geometrical and mechanical properties of viral capsids

	a (nm)	h (nm)	E (GPa)	D (k_BT)
HBV[4]	14.22	2.24	0.26	70.5
CCMV[4]	11.8	2.8	0.14	74.2
Bacteriophage λ[4]	30	1.8	1	140.8
MVM[4]	12.5	2	1.25	241.4
Mature HIV[29]	50	5	0.44	1330
HSV1 (ref. 4)	49.5	4	1	1540
Mature MLV[30]	50	4	1.027	1590

Thin-shelled solid capsules made of hyperelastic materials can undergo large deformation (both bending and stretching). Therefore, hyperelastic capsules under membrane wrapping are expected to display an intermediate extent of bending and stretching between those of linear elastic solid capsules and fluid vesicles. As a result, the wrapping phase diagrams for hyperelastic capsules would be somewhere in between those for linear elastic capsules (Fig. 4) and for vesicles (Fig. 3b–e in ref. 12). Since the particles are expected to deform and equilibrate on a time scale much smaller than that of cell uptake which typically requires relatively long range diffusive transport of receptors along the cell membrane, the cell-particle system can be assumed in a static state of minimum energy during cell uptake. It would be interesting and challenging to investigate the cell uptake of viscoelastic capsules whose relaxation time scales are comparable to the time scale of receptor diffusion in cell membranes.[35] A size-dependent uptake behavior can also be expected based on earlier studies on rigid nanoparticles.[35–39]

The conclusion that stiff particles can achieve full wrapping more easily than soft ones has been obtained for both solid capsules (Fig. 4) and fluid vesicles,[7,12] confirming our previous conjecture that this conclusion should be generic and not specific to the specific particle model.[12] The elasticity effect on cellular uptake has important implications on therapeutic drug delivery. Soft thin-shelled capsules require larger adhesion energy to reach full wrapping and should lead to a longer circulating time than stiff capsules. The stiffness of solid capsules can be tuned over a wide range by many methods such as varying the shell thickness, using materials of different compositions and changing degrees of cross-linking.[1,2] Since the circulating time depends on capsule stiffness, the latter can thus be tuned to adjust the former into a specific therapeutic time window of drug delivery. The same strategy of tuning the bending stiffness of nanoparticles can also be applied to vesicles such as liposomes whose membrane bending stiffness can be tuned by adjusting the cholesterol content.[27] Therefore, it should be possible to control the therapeutic time in drug delivery using liposome-based nanocapsules with liposomal subcompartments, called capsosomes, which can be fabricated by a layer-by-layer approach.[40,41] By tuning the properties of the capsule shell and interior liposome membrane, capsosomes can enhance the protection of liposomal subcompartments and achieve sequenced drug release.

In some cases, singular therapies might not be as beneficial as proposed due to the development of drug resistance by target cells. To overcome this disadvantage, researchers have developed drug delivery systems of multiagent chemotherapy to improve the delivery efficiency. For example, liposomes containing erlotinib and doxorubicin have been designed to enhance the tumor killing efficiency through the primary release of the lipid-soluble bilayer-embedded erlotinib which in turn sensitizes tumor cells to subsequent exposure to cytotoxic doxorubicin encapsulated in liposomes.[42] A similar strategy can be employed for capsosomes, in which multiple types of drugs are loaded such that both the prevenient facilitating drugs and liposomal subcompartments are encapsulated in capsules while drugs aiming for subsequent exposure are loaded in the liposomal subcompartments. Cell

uptake tuned by stiffness is expected to provide a possible approach to designing controlled, efficient and effective drug delivery and release systems.

5 Conclusions

A theoretical study has been performed on cell uptake of linear elastic thin-shelled solid nanocapsules. In this study, the deformation of the capsule and cell membrane is modeled in a coupled Lagrangian–Eulerian description. The interior point method was employed to optimize the system energy, then results were obtained on the corresponding morphologies of the nanocapsule and cell membrane, and finally the wrapping phase diagrams were determined to describe transition boundaries between different wrapping phases. The wrapping phases exhibit strong dependence on the size of nanocapsules, adhesion energy, membrane tension, and bending rigidity ratio between the capsule and membrane. It has been found that stiffer nanocapsules require less adhesion energy to achieve full wrapping than softer ones. This result is also valid in the case of cell uptake of fluid vesicular nanoparticles such as liposomes.[12] Further calculations indicated that the elastic energy change in the case of cell uptake of nanocapsules with bending rigidity D is larger than that for vesicles with the same bending stiffness $\kappa_v = D$, and the energy distinction becomes especially significant in the case of very soft nanoparticles. This result suggests that nanocapsules with bending rigidity D can achieve full wrapping more easily than vesicles with the same bending stiffness $\kappa_v = D$; and the softer the particles, the more distinct this effect. The elasticity effects on cell uptake of nanocapsules and vesicles should have broad implications for drug delivery systems. Several methods capable of tuning the particle elasticity and sequence of drug release can be suggested to control cellular uptake and therapeutic efficiency.

Further studies on cell uptake of solid capsules could take into account other constitutive laws for capsules,[43] effects of capsule thickness, shape,[36,39,44–47] surface properties,[13,48] residual stress or pre-stress in capsules, and constraints such as given capsule pressure or volume.[5–7] The optimization method based on B-spline parameterization can be immediately employed in the studies of adhesive contact between thin shell structures and rigid or elastic substrates,[21,22,49–51] micropipette aspiration of elastic capsules or vesicles, axisymmetric indentation on thin films and other cases displaying axisymmetric configuration.

Acknowledgements

Support from the National Science Foundation under INSPIRE: "Computational Design for the Safe Development of High-Aspect-Ratio Nanomaterials", CBET-1344097, and one of its predecessor grants, CMMI-1028530, is gratefully acknowledged.

References

1 C. S. Peyratout and L. Dähne, *Angew. Chem., Int. Ed.*, 2004, **43**, 3762–3783.
2 C. E. Mora-Huertas, H. Fessi and A. Elaissari, *Int. J. Pharm.*, 2010, **385**, 113–142.
3 T. S. Baker, N. H. Olson and S. D. Fuller, *Microbiol. Mol. Biol. Rev.*, 1999, **63**, 862–922.
4 W. H. Roos, R. Bruinsma and G. J. L. Wuite, *Nat. Phys.*, 2010, **6**, 733–743.
5 S. Knoche and J. Kierfeld, *Phys. Rev. E: Stat., Nonlinear, Soft Matter Phys.*, 2011, **84**, 046608.
6 S. Knoche and J. Kierfeld, *Soft Matter*, 2014, **10**, 8358–8369.
7 X. Yi and H. Gao, *Phys. Rev. E: Stat., Nonlinear, Soft Matter Phys.*, 2014, **89**, 062712.
8 M. F. Bédard, A. Munoz-Javier, R. Mueller, P. del Pino, A. Fery, W. J. Parak, A. G. Skirtach and G. B. Sukhorukov, *Soft Matter*, 2009, **5**, 148–155.
9 M. Delcea, S. Schmidt, R. Palankar, P. A. L. Fernandes, A. Fery, H. Möhwald and A. G. Skirtach, *Small*, 2010, **6**, 2858–2862.
10 R. Palankar, B.-E. Pinchasik, S. Schmidt, B. G. De Geest, A. Fery, H. Möhwald, A. G. Skirtach and M. Delcea, *J. Mater. Chem. B*, 2013, **1**, 1175–1181.
11 K. A. Beningo and Y. L. Wang, *J. Cell Sci.*, 2002, **115**, 849–856.
12 X. Yi, X. Shi and H. Gao, *Phys. Rev. Lett.*, 2011, **107**, 098101.
13 H.-M. Ding and Y.-Q. Ma, *Biomaterials*, 2012, **33**, 5798–5802.
14 R. Guo, J. Mao and L.-T. Yan, *ACS Nano*, 2013, **7**, 10646–10653.
15 T. R. Powers, G. Huber and R. E. Goldstein, *Phys. Rev. E: Stat., Nonlinear, Soft Matter Phys.*, 2002, **65**, 041901.
16 A. Libai and J. G. Simmonds, *The Nonlinear Theory of Elastic Shells*, Cambridge University Press, Cambridge, 2nd edn, 1998.
17 W. Helfrich, *Z. Naturforsch., C: Biochem., Biophys., Biol., Virol.*, 1973, **28**, 693–703.
18 M. Deserno, *Phys. Rev. E: Stat., Nonlinear, Soft Matter Phys.*, 2004, **69**, 031903.
19 G. Farin, *Curves and Surfaces for CAGD: a Practical Guide*, Morgan Kaufmann, San Francisco, 5th edn, 2002.
20 J. Nocedal and S. J. Wright, *Numerical Optimization*, Springer, New York, 2nd edn, 2006.
21 R. M. Springman and J. L. Bassani, *J. Mech. Phys. Solids*, 2008, **56**, 2358–2380.
22 S. Komura, K. Tamura and T. Kato, *Eur. Phys. J. E*, 2005, **18**, 343–358.
23 J. Huang, M. Juszkiewicz, W. H. de Jeu, E. Cerda, T. Emrick, N. Menon and T. P. Russell, *Science*, 2007, **317**, 650–653.
24 J. Hure, B. Roman and J. Bico, *Phys. Rev. Lett.*, 2011, **106**, 174301.
25 T. M. Allen and P. R. Cullis, *Adv. Drug Delivery Rev.*, 2013, **65**, 36–48.
26 E. Kreyszig, *Differential Geometry*, Dover Publications, New York, 1991.
27 P. Méléard, C. Gerbeaud, T. Pott, L. Fernandez-Puente, I. Bivas, M. D. Mitov, J. Dufourcq and P. Bothorel, *Biophys. J.*, 1997, **72**, 2616–2629.
28 I. A. T. Schaap, F. Eghiaian, A. des Georges and C. Veigel, *J. Biol. Chem.*, 2012, **287**, 41078–41088.
29 N. Kol, Y. Shi, M. Tsvitov, D. Barlam, R. Z. Shneck, M. S. Kay and I. Rousso, *Biophys. J.*, 2007, **92**, 1777–1783.

30 N. Kol, M. Gladnikoff, D. Barlam, R. Z. Shneck, A. Rein and I. Rousso, *Biophys. J.*, 2006, **91**, 767–774.
31 Z. Wang, A. A. Volinsky and N. D. Gallant, *J. Appl. Polym. Sci.*, 2014, **131**, 41050.
32 L. A. Fiel, L. M. Rebêlo, T. M. Santiago, M. D. Adorne, S. S. Guterres, J. S. de Sousa and A. R. Pohlmann, *Soft Matter*, 2011, **7**, 7240–7247.
33 Y. Wei, B. Wang, J. Wu, R. Yang and M. L. Dunn, *Nano Lett.*, 2013, **13**, 26–30.
34 J. Wu, B. Wang, Y. Wei, R. Yang and M. Dresselhaus, *Mater. Res. Lett.*, 2013, **1**, 200–206.
35 H. Gao, W. Shi and L. B. Freund, *Proc. Natl. Acad. Sci. U. S. A.*, 2005, **102**, 9469–9474.
36 B. D. Chithrani, A. A. Ghazani and W. C. W. Chan, *Nano Lett.*, 2006, **6**, 662–668.
37 S. Zhang, J. Li, G. Lykotrafitis, G. Bao and S. Suresh, *Adv. Mater.*, 2009, **21**, 419–424.
38 H. Yuan, J. Li, G. Bao and S. Zhang, *Phys. Rev. Lett.*, 2010, **105**, 138101.
39 H. Gao, *J. Mech. Phys. Solids*, 2014, **62**, 312–339.
40 B. Städler, R. Chandrawati, K. Goldie and F. Caruso, *Langmuir*, 2009, **25**, 6725–6732.
41 R. Chandrawati, Ph.D. thesis, University of Melbourne, 2011.
42 S. W. Morton, M. J. Lee, Z. J. Deng, E. C. Dreaden, E. Siouve, K. E. Shopsowitz, N. J. Shah, M. B. Yaffe and P. T. Hammond, *Sci. Signaling*, 2014, **7**, ra44.
43 C. Pozrikidis, *Modeling and Simulation of Capsules and Biological Cells*, Chapman & Hall/CRC, Boca Raton, 2003.
44 S. Dasgupta, T. Auth and G. Gompper, *Soft Matter*, 2013, **9**, 5473–5482.
45 A. H. Bahrami, *Soft Matter*, 2013, **9**, 8642–8646.
46 X. Shi, A. von dem Bussche, R. H. Hurt, A. B. Kane and H. Gao, *Nat. Nanotechnol.*, 2011, **6**, 714–719.
47 X. Yi, X. Shi and H. Gao, *Nano Lett.*, 2014, **14**, 1049–1055.
48 Y. Li, M. Kröger and W. K. Liu, *Biomaterials*, 2014, **35**, 8467–8478.
49 K.-T. Wan and K.-K. Liu, *Med. Biol. Eng. Comput.*, 2001, **39**, 605–608.
50 R. M. Springman and J. L. Bassani, *J. Mech. Phys. Solids*, 2009, **57**, 909–931.
51 J. Lin, Y. Lin and J. Qian, *Langmuir*, 2014, **30**, 6089–6094.